Chapter 3

Novel Desalination RO Membranes

Amira Abdelrasoul, Huu Doan and Ali Lohi

Additional information is available at the end of the chapter

http://dx.doi.org/10.5772/intechopen.71719

Abstract

Since the initial operation of the first reverse osmosis (RO) desalination plants, only polymeric membranes have been employed for industrial use. As described in the previous chapter, the various advancements in the conventional polymeric RO membranes have been rather limited since the late 1990s, especially in the membrane permeability issue. Although new membrane modules have been released, however most of them are improved through a method that relies on increasing the membrane area per module. Recently, advances in nanotechnology have led to the development of nanostructured materials which may form the basis for new RO membranes. Li and Wang have included inorganic membranes and thin film nanocomposite membranes in a recent review, whereas Mauter and Elimelech have discussed the potential of carbon nanotube membranes for use as high flux membrane filters. In this chapter, the development of membranes that have been discussed in the previous two reviews will be briefly highlighted with a particular focus on the possibility of them being engineered into commercial RO membranes. At the same time this chapter includes a discussion about structured polymeric membranes synthesized via a new course featuring carbon-derived nanoporous membranes and biomimetic membranes. The coverage of all proposed novel desalination RO membranes in this section is aimed to provide a general overview of these materials and to draw a fair comparison of them possibly being developed into commercial RO membranes.

Keywords: polymeric membrane, reverse osmosis, mixed matrix membranes, inorganic membrane, nanoporous membranes

1. Introduction

Since the initial operation of the first reverse osmosis (RO) desalination plants, only polymeric membranes have been employed for industrial use [1, 2]. As described in the previous chapter, the various advancements in the conventional polymeric RO membranes have been rather limited since the late 1990s, especially in the membrane permeability issue. Although

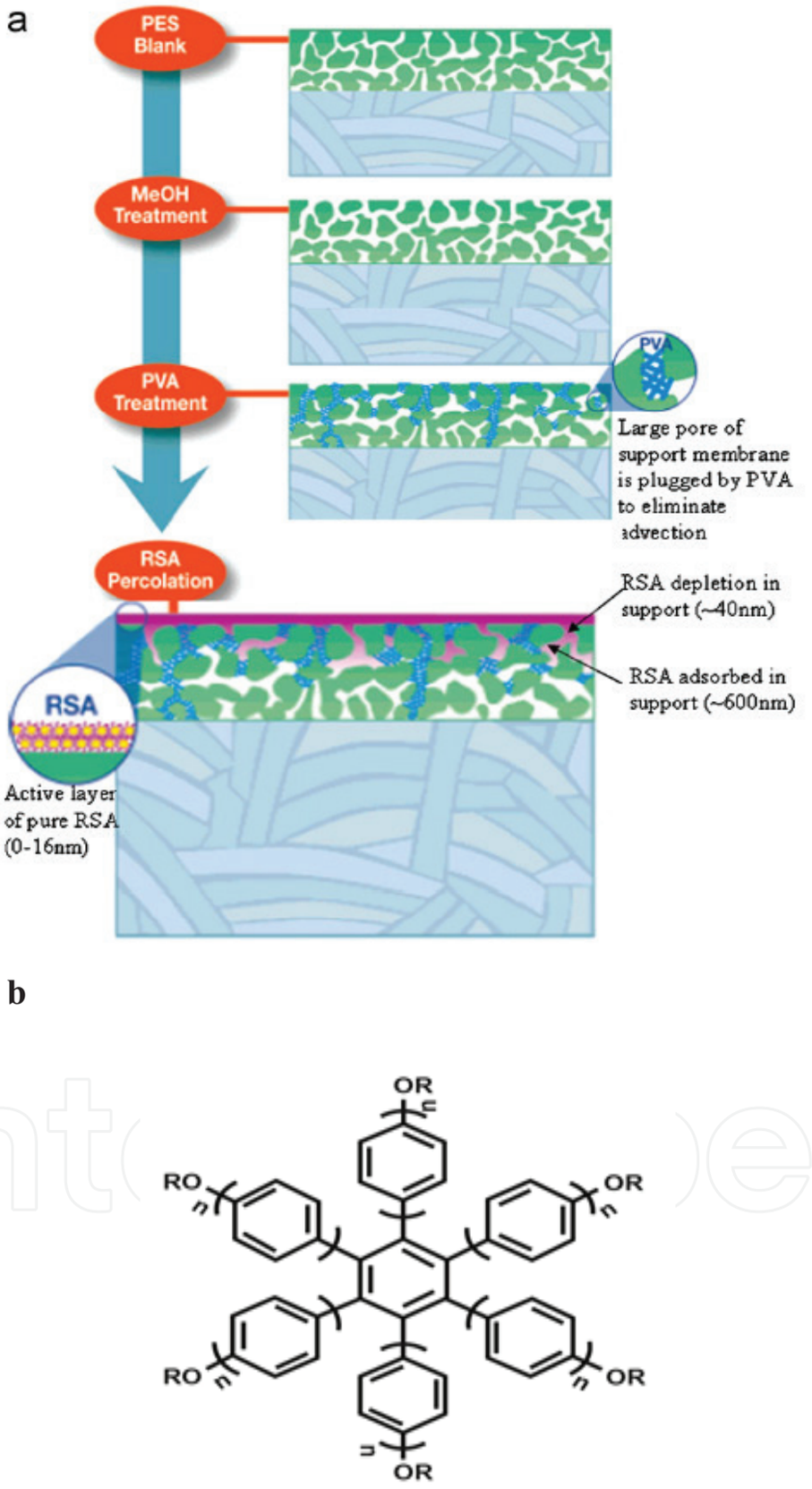

Figure 1. (a) RSA membrane synthesis process and (b) one of the RSA molecules tested [3].

a number of new membrane modules have been designed and tested, the majority of these are enhanced using a methodology that is reliant on the augmentation of the membrane's area per module. Developments in recent nanotechnology research have contributed to the creation of nanostructured materials that may prove to be a more effective basis for new types of RO membranes. For instance, Li and Wang research collaborative have focused on thin-film nanocomposite membranes and inorganic membranes in a recent overview, while Mauter and Elimelech examined at the possibilities of implementing carbon nanotube (CNT) membranes as high-flux membrane filters [1, 2]. This chapter outlines the evolution of membranes that have been discussed in the previous two reviews and briefly interrogates the possibility of these designs being engineered into successful commercial RO membranes. Furthermore, this chapter begins a critical discussion on the structured polymeric membranes synthesized using innovative course based on biomimetic membranes and carbon-derived nanoporous membranes. In this section, the covered methods of proposed desalination of RO membranes aim to offer a broader summary of membrane materials and outline the comparative potential of them being developed into viable commercial RO membranes.

2. Polymeric membrane created using rigid star amphiphiles

Recent research report has noted the development of a nanofiltration (NF) membrane based on rigid star amphiphiles (RSAs) [3, 4]. As shown in **Figure 1(a)**, nanofiltration membranes were created using percolation of methanol solutions of the RSAs and through an asymmetric polyethersulfone support that had been conditioned earlier with crosslinked poly-vinyl alcohol and methanol. **Figure 1(b)** illustrates one of the RSA molecules synthesized with the help of diverse cyclization methods as membrane-building block materials.

During atomic force microscopy (AFM) and scanning electron microscopy (SEM) analysis, the membrane showed an exceedingly smooth surface with an average roughness values within the range of 1–2 nm. Notably, this roughness potential is quite distinct from the roughness values found in commercially available NF membranes (20–70 nm). The RSA membrane barrier layer is extremely thin and features a thickness of around 20 nm. This composite multi-layer dendrimer arrangement helps regulate the narrower pore size distribution. When compared to the commercially available NF membranes, these membranes have exhibited similar contaminants rejection performances, but with doubled flux values. This newer approach to polymeric membrane synthesis can provide a superior alternative for tuning membrane structure, when considering polymeric NF and RO membranes' morphological similarities. Further research is still crucial when it comes to definitively verifying the method's suitability for the RO process. Specifically, the membrane's salt rejection potential has remained unspecified.

3. Ceramic/inorganic membranes

The ceramic types of membranes are primarily created using silica, alumina, zirconia, titania, or a combination of these materials. Because of their substantially higher manufacturing

costs, the application of ceramic membranes is presently limited to cases where polymeric membranes cannot be properly used, such as in processes involving radioactives/heavily contaminated feeds, highly reactive environments, and elevated operating temperatures [5]. In most cases, ceramic membranes are based on a meso- or micro-porous active layer and a macro-porous support layer. The current top techniques for ceramic membrane production include paste extrusion for its supports, as well as powder suspensions slip-casting or the sol–gel processing of colloidal suspensions for active layer deposition. Ceramic membrane's foundational elements have been created using tubular modules that have been converted into monolithic honeycomb structures capable of providing much higher packing potential and efficiency. At this point, commercialized ceramic membranes are implemented extensively in micro- and ultra-filtration applications. On the other hand, ceramic membranes that can be used for successful nanofiltration still require further development and testing [6].

The industrial-scale application of ceramic-type membranes in domestic water production settings is uncommon; however, the membrane's overall process sturdiness has gained attention of researchers for purposes of pervaporation [9] and membrane distillation [7, 8]. A group of researchers from the New Mexico Institute of Mining and Technology have recently reported on the potential applications of ceramic membranes for RO desalination processes [10]. Due to the advantages of desalting oil field water, and inspired by molecular dynamic simulation results that showcased 100% of ion rejection potential in all-Si ZK-4 zeolite-type membranes [11], this research collaborative has conducted an experiment-based examination of the RO separation mechanism as well as assessed the viability of using ceramic membranes. The sub-nm inter-crystalline pores of the zeolite structure allowing for the rejection of the salt and passage of water molecules are outlined in **Figure 2** [12]. Theoretical sets of calculations suggest that ions can be completely rejected by zeolite membranes if they have pore sizes smaller than the hydrated ion's size. A-type zeolite membranes have 0.4-nm size pores and MFI-type membranes of 0.56-nm pore diameters. The first experimental attempt at developing an RO of an NaCl solution with the aid of the MFI silicalite-1 zeolite membrane represented a 77% salt rejection potential and a water flux as low as 0.003 $m^3\ m^{-2}\ day^{-1}$ at 21 bar. It was similarly noted that the rejection potential of bivalent cations was greater than for monovalent ions in a test environment that implemented a feed including mixed ion species. As a consequence, the rejection of sodium ions in a mixed ion solution was smaller than the one occurring in a pure solution of NaCl. These data indicate that the filtration mechanism relies on, both, the size exclusion potential and the Donnan exclusion created by the charged double layer produced by adsorbed ions on the intercrystalline walls or the pore [13].

New research has been undertaken to improve the results by modifying the zeolite structure, despite the fact that the first RO tests with a zeolite membrane failed and, both, water flux and salt rejection values were far too low for practical industrial applications. The Si/Al ratio, which tends to dictate the membrane's surface charge and wettability parameters, has been enhanced to offer better salt rejection and flux. The Al content within the membrane can noticeably modify the surface hydrophilicity and, as a consequence, its affinity with water [14]. The flaws of the crystal structure can be minimized using a secondary growth of a zeolite layer on top of the zeolite placed onto a porous α-alumina substrate [15]. A combinatory approach such as this produced a significant improvement during testing of a 2-μm thick

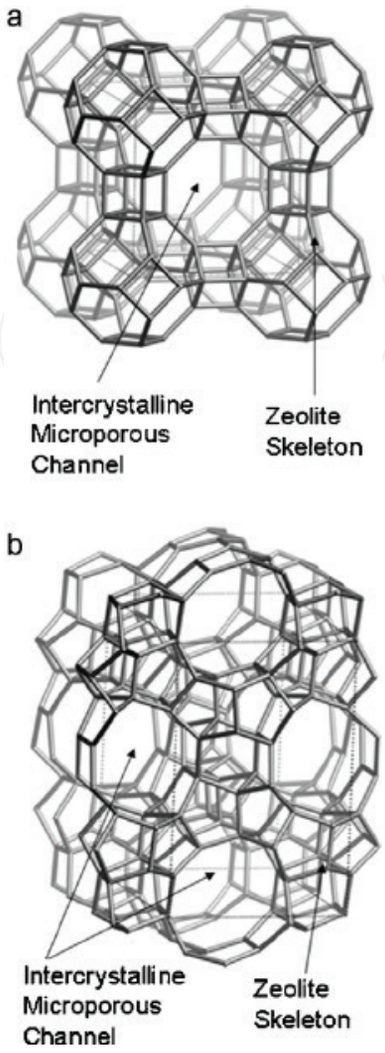

Figure 2. Micro-porous ceramic membrane structure: micro-porous channel in the crystalline structure (a) Type A zeolite and (b) MFI zeolite (reprinted with permission from Baerlocher et al. [12]).

zeolite membrane with 50:50 Si/Al ratio that rejected 92.9% of sodium ions and offered a water flux value of 1.129 $kgm^{-2}\ h^{-1}$ at 28 bar [16]. The same research tests were able to further reduce the thickness of the membrane to 0.7 μm, thus ensuring outstanding salt rejection (97.3%) and organic values (>99%), and obtaining a permeate flux improved by almost four times [17, 18].

Although innovation in the zeolite membranes research has shown substantial progress in the last 10 years, their economical viability and overall performance do not yet compare to that of the polymeric membranes. On the downside, the zeolite membrane thickness value is at least three times greater than the current quality polymeric RO membrane, and this creates higher overall resistance to permeate flux. As a consequence, ceramic-type membranes require a membrane area that is at least 50 times larger, than would be necessary in the polymeric counterpart, in order to reach similar production capacity. This membrane area parameter may even be greater if the lower-packing effectiveness and increased density are taken into consideration. Although zeolite membranes are intended to allow for higher organic rejection potential, organic fouling has produced almost 25% loss in flux capacity

after only 2 h of operation, even though full recovery of flux was eventually achieved with the help of chemical washing [18]. The higher-salinity feeds are projected to cause shrinkage of the double layer because of the counter ions screening effect on the surface charge values. Thus, an unwanted growth in effective intercrystalline pore sizes can incite ion transport and then lower the rejection efficiency. These experimental tests were conducted with a low NaCl concentration (0.1%) and standard seawater desalination tests at 3.5% NaCl and must be further examined so as to assess their potential application for desalination of oil field seawater.

Another possible candidate for the formation of sub-nm porous materials is carbon. A carefully controlled carbide-derived carbon (CDC) materials' pore size distribution has been formerly reported in research studies [19]. There are several advantages to carbon since CDC allows for enhanced shape, control of pore size, and uniformity. For instance, these advantages can be seen in the manipulation of chlorination temperatures as indicated in **Figure 3**. Likewise noted was the synthesis of CDC membranes through the creation of a thin CDC film on top of the porous ceramic support [20]. This initial research study offers a method of developing asymmetric CDC membranes with an average pore size of about 0.7 nm, as well as of showcasing the potential for effective monovalent salt exclusion. Further research testing is crucial in order to assess the practicality and feasibility of CDC membranes for applications in long-term RO desalination settings.

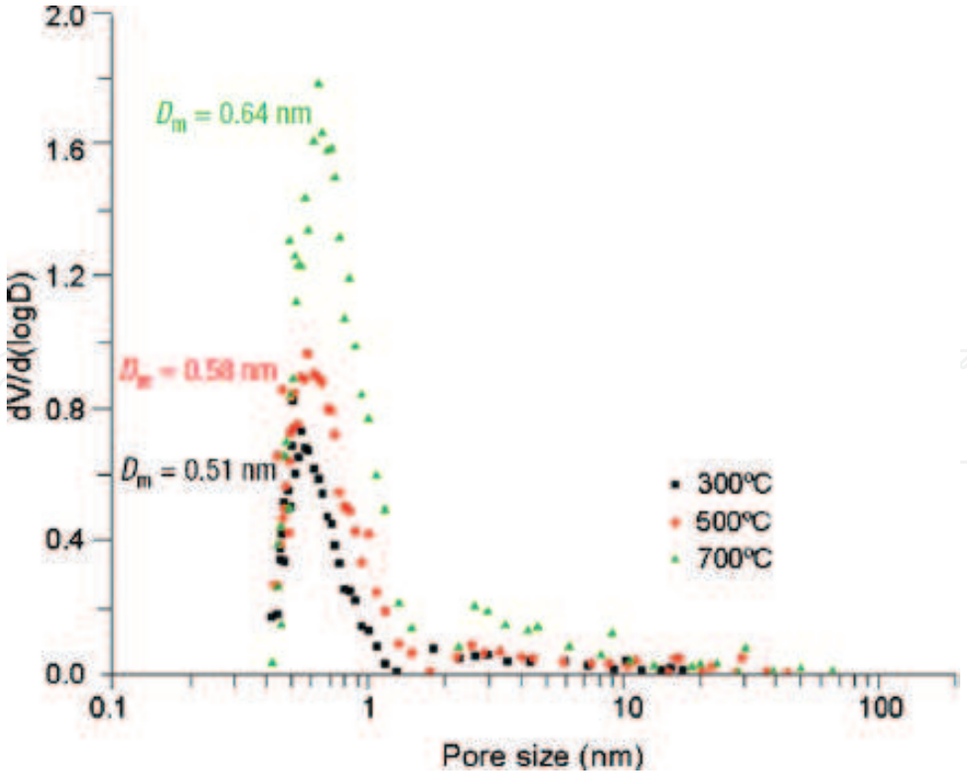

Figure 3. Differential pore size distribution for CDC-synthesized membrane at varying chlorination temperatures measured by methyl chloride adsorption (reprinted with permission from Gogotsi et al. [19]).

4. Mixed matrix membranes

The theoretical framework behind mixed matrix membranes (MMM), is the mixing of inorganic and organic materials and is not quite recent. In 1980, Universal Oil Product (UOP) created a silicalite-cellulose acetate MMM for the purposes of gas separation which showed advanced selectivity potential when compared to the more conventional polymeric membranes [21]. Even though MMMs were made for water/ethanol separation using pervaporation in the 1990s, the inclusion of inorganic materials as part of the organic RO thin-film composite (TFC) membranes and TFC membranes began in the early part of 2000s [22]. The primary aim of MMM is to efficiently merge the potential benefits offered by either material. In particular, there is a need to combine advantages such as good permselectivity, long operational experience, and higher packing density of the polymeric membranes, together with the improved biological, thermal, and chemical stability offered by the inorganic membranes [23].

4.1. Nanoparticle/polymeric membranes

In a wide range of industries, the synthetic membranes are becoming a key technology in separation processes and their applications. In most cases, the synthetic membranes are made out of organic materials like polymers, and inorganic materials like ceramics. Currently ongoing membrane research primarily looks at polymeric membranes because of their greater flexibility, smaller spaces required for installation, improved control over the pore-forming mechanisms, and comparatively smaller costs. In combination, these properties make the polymeric membranes a more suitable material in a variety of applications. However, frequent issues that researchers focus on when it comes to polymeric membranes are exposure to biofouling, lower fluxes, inferior mechanical strength, and higher hydrophobicity. The adding of nanoparticles into polymeric membranes became a key trend in the recent membrane research studies. Arguably, the insertion of nanosized materials may be able to incite synergistic effects when combined with diverse material types [24].

Iron is the most abundant transition metals as well as the fourth most available element in the earth's crust, qualities that make it the pillar of modern infrastructure. In fact, as a type of nanoparticle, iron has been overlooked in comparison to oxides and other metals like nickel, gold, platinum, and cobalt. Although this is an unfortunate limitation, there is an explicit reason for it. While iron's reactivity can be a key quality for macroscopic applications, especially rusting, it becomes a concern at the nanoscale levels. The fact that finely divided iron is pyrophoric is one of the main reasons responsible for iron nanoparticles not being more researched or applied. Such a severe reactivity potential has habitually made iron nanoparticles challenging to study and difficult to apply practically. On the other hand, iron has many properties to offer at the nanoscale, such as its catalytic and strong magnetic properties. In the recent research studies, iron's potential is being explored more rigorously, especially in relation to the membrane separation processes, which are discussed here.

As already noted, excessive reactivity of the iron metal makes it unfitting for application as pure metal nanoparticles [24]. As a result, instead of the pure iron nanoparticles, iron compounds are integrated into the polymeric membranes. The inclusion of iron compounds

nanoparticles helps improve membrane performance with regard to some of their specific uses. Nafion is one of the polymeric membranes integrated with iron compounds. Specifically, Nafion is a sulfonated tetrafluoroethylene-based fluoropolymer-copolymer, and a first type in the synthetic polymers class featuring ionic properties, namely ionomers. Due to its superior thermal and mechanical stability, Nafion received much attention as a proton conductor used in proton exchange membrane (PEM) fuel cells. Films based on Nafion are effective as proton-conducting membranes in the case of direct methanol fuel cells (DMFCs). On the other hand, unmodified Nafion membranes usually have higher methanol permeability and this effectually makes them unsuitable for uses for the production of commercial-type fuel cells [25]. Therefore, the inclusion of nanoparticles featuring highly acidic and inorganic materials into Nafion membranes was shown to be the most effectual method for lowering methanol permeability potential [26–32]. Incorporating nanomaterials with greater surface acidity helps produce higher proton conductivity composite membranes, and the particle blocking of pores decreases methanol transport potential.

Inside the pores of Nafion membranes, the sol–gel synthesis of inorganic phases (SiO_2, TiO_2, ZrO_2) has been found as a successful modification direction that allows obtaining higher selectivity values [32–35]. Zeolites are also used as modifiers in Nafion membranes, primarily because of their high surface acidity, greater water intake values, and intrinsically narrow pore size distributions [36]. Recent research project reported results of methanol transport properties in a number of Nafion-composite membranes integrating micro- and nanosized zeolite particles (Fe-silicate-1), in situ crystallized Fe-silicalite-1, and amorphous silica, comparable to the unmodified commercial nafion-115-type membranes [25]. During the development of the composites, a supercritical carbon dioxide treatment was applied to some of the membranes before the integration of the inorganic phase. In this case, two approaches to zeolites deposition were used, specifically, direct in situ synthesis inside the pores of Nafion membrane and deposition from colloid or suspension solution. Relatively low methanol permeability potential was achieved in composite-type membranes created with the aid of the colloidal intercalation route (from colloidal Fe-sillicate-1 and silica solution), as well as using the in situ synthesis of Fe-silicate-1 inside the Nafion membrane's pores. In order to change its structure, supercritical CO_2 activation of a Nafion membrane before the zeolites deposition was implemented. The developed Nafion-zeolite composite membranes indicated a substantial reduction in methanol permeability, if colloidal rather than suspended Fe-silicalite-1 particles were used for deposition. Furthermore, there was a 19-fold greater selectivity value if compared to pure commercial Nafion-115 membrane or composite membranes made without previous supercritical treatment. The approach of in situ synthesis of zeolite inside the membrane's pores was determined to be quite successful for the production of composites and ensured a sixfold greater selectivity potential for the composite membrane, if compared to pure Nafion [25]. Iron compounds are likewise integrated into other polymeric membranes so as to create proton exchange membranes, in addition to iron's use with Nafion membranes and the reduction of methanol permeability. Further research has been recently done on the production of ion-conducting membranes by self-assembly of surface-charged nanoparticles [37]. Researchers suggest that the membranes created using closely packed nanoparticles offered noticeably greater proton conductivity if compared to

solution-cast films of similar ion-exchange capacity (IEC) and composition. Nonetheless, there was a degree of limitation on maximum IEC, since high-IEC membranes showcased extreme swelling in water and thus substantially deterred the testing for proton conductivity. Membranes featuring proton-conducting particles constructed in a suitable matrix may be designed in a manner that avoids these issues. In particular, the particles could be carefully aligned to gain the percolation necessary for proton conduction, while the swelling in methanol or water can be supervised through the selection of a water-resistant matrix. Another research project outlines the synthesis of composite particles with sulfonated crosslinked polystyrene (SXLPS) intended for use in the proton exchange membranes and ribbed fuel cells [38]. In this instance, the approach implemented for polymerization was comparable to the mini-emulsion polymerization described by Ramirez et al. [39]. Admittedly, a number of procedure modifications were necessary for the production of functional and crosslinked polymer-iron oxide composites. Researchers likewise reported a membrane production process that requires the alignment of synthesized particles in a high-performance sulfonated poly(etherketoneketone) (SPEKK) matrix [40] and offers a number of properties of PEMs for fuel cell uses. The membrane's ultimate properties depended on a range of aspects, including the matrix, size of particles, and the particle's IEC. The primary aim of this research project was to show an applicable membrane-fabrication method that can be used to improve the PEMs' overall conductivity. As noted [38], the composite ion-conducting nanoparticles were synthesized with the help of emulsion polymerization. The particles' polymeric component contained sulfonated crosslinked polystyrene as well as the inorganic component of γ-Fe_2O_3. As a result of the experimental runs, a particle synthesis method was compiled so as to elucidate the abnormal morphologies of composite particles. The distribution breadth increased with sulfonated content, while the average synthesized particles' diameter value correlation to changing feed compositions were within the range of 230–340 nm (**Figure 4**).

Titanium oxide (TiO_2) is a relatively common photocatalytic material that has been frequently employed for decomposition and disinfection of various organic compounds [41]. This potentially dual property makes TiO_2 a compelling anti-fouling coating option. The anatase TiO_2 nanoparticles (<10 nm) are prepared using the process of controlled hydrolysis of titanium tetraisopropoxide. These particles are then dip-coated as an interfacially polymerized fully crosslinked polyamide TFC membrane with a surface layer further functionalized with carboxylate groups [42]. Notably, these carboxylate groups are essential for the TiO_2 self-assembly within the barrier layer and require the use of an adsorption mechanism. Experimental testing based on an *Escherichia coli* containing feed water has shown improved anti-biofouling properties. In fact, these improvements aided with UV excitation and did not compromise the salt rejection and flux performance of the original membrane and its properties. There was no substantial loss of TiO_2 nanoparticles from the membrane notes after a continuous 7-day RO research trial run [42, 43].

Moreover, zeolite nanoparticles have been used similarly during the preparation of MMMs (**Figure 5**). The first step in this process is for the zeolite nanoparticles to be synthesized with the help of a templated hydrothermal reaction. What follows are a series of difficult processes that involve carbonization, sodium exchange, template removal, and calcination [44]. The formed NaA-type zeolite particles appear to be within the size range of 50–150 nm and feature an Si/Al

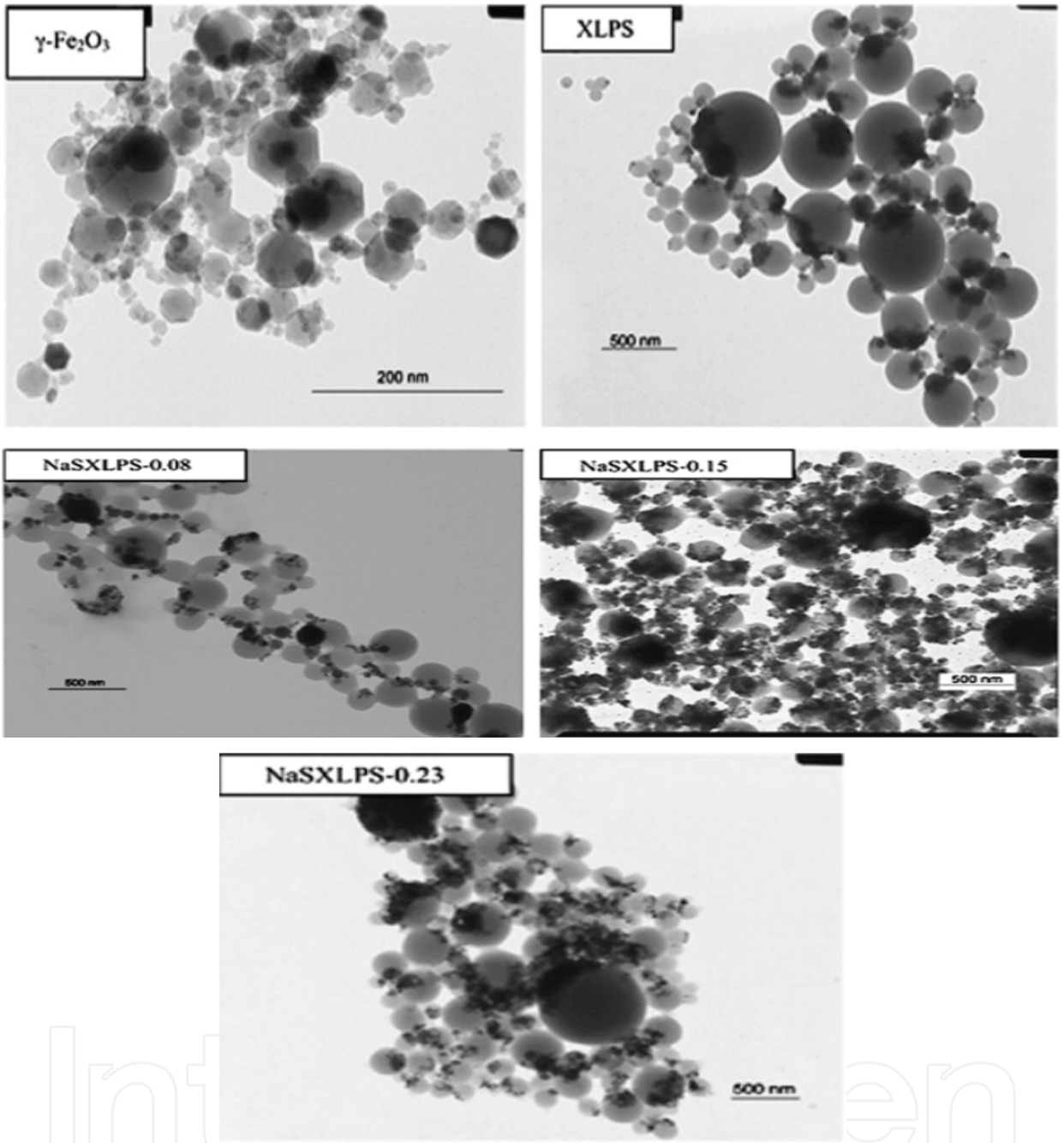

Figure 4. TEM images of the starting material γ-Fe2O3 and synthesized crosslinked polystyrene γ-Fe2O3 particles. Adapted from Ref. [24].

ratio of 1.5. Reports suggest that these particles are highly hydrophilic (contact angle of <5°) and have negatively charged 0.4-nm pores that repulse anions. Before the interfacial polycondensation reaction can occur, the zeolite nanoparticles are dissolved into a crosslinking agent solution, such as trimesoyl chloride dissolved in hexane. This method differs from the approach based on dipping the previously made membrane into a nanoparticle-containing solution, as occurs with the TiO_2 nanocomposite-type membranes. In this case, a homogeneous zeolite particle dispersion is created using ultrasonication, prior to the enactment of the standard interfacial polymerization

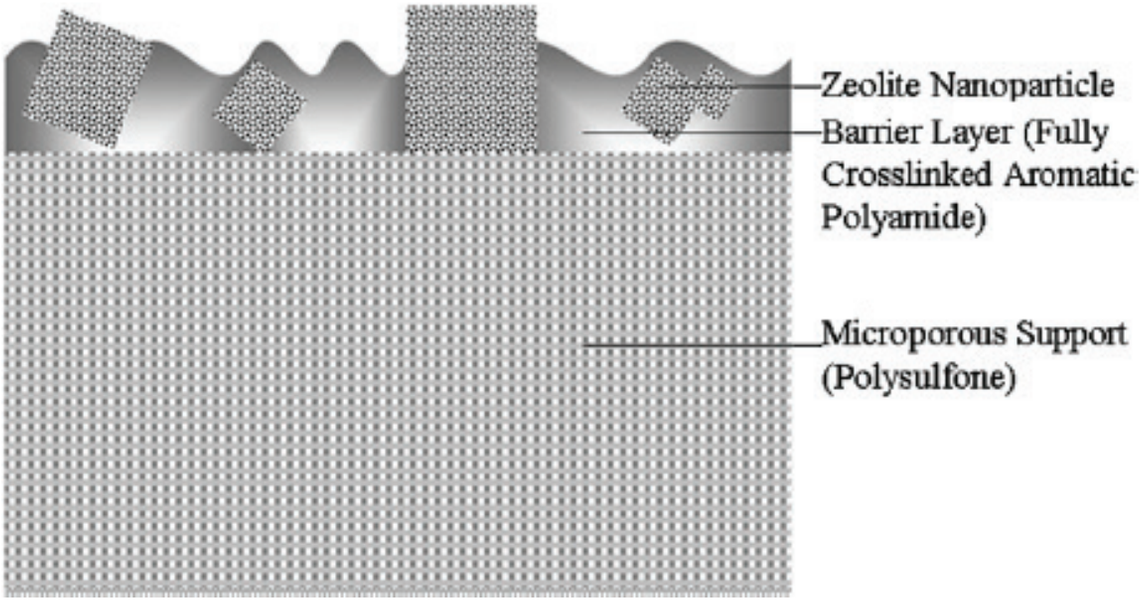

Figure 5. Schematic cross-section of zeolite nanocomposite membrane (reprinted with permission from Jeong et al. [44]).

process. During this experiment, the RO membranes with a variety of zeolite-loading values were prepared and the subsequent changes in the membrane's properties were examined. For instance, the membranes became smoother in quality, more negatively charged with increasing nanoparticle loading, and more hydrophilic. Relative to the hand-cast TFC membranes without zeolite nanoparticles, the MMM membranes showed 90% of flux and a minor increase in the salt rejection potential. Researchers indicate that this could be due to the changes in membrane morphology and improved Donnan exclusion with regard to zeolite particles [44, 45]. The altered surface properties and membrane's new separation performance facilitated by the variations in zeolite nanoparticle loading are shown in **Figure 6**.

4.2. Carbon nanotube/polymeric membranes

A number of researchers begun to pay closer attention to carbon nanotubes because of the resemblance between their fluid transport characteristics and the water transport channels in biological type of membranes [46]. Successful experimental instance of fluid flow in a CNT membrane was first observed in 2004 [47]. For this experiment, well-aligned multi-wall CNT membranes were created with the aid of catalytic chemical vapor deposition (CCVD) situated on the surface of quartz substrates. These membranes were then spun coated with polystyrene in order to effectively cover inter-tube gaps, while plasma etching was employed to open the CNTs' tips. An experimental assessment of water transport in a solid polystyrene film membrane that includes 7-nm diameter multi-wall CNTs indicates that the detected flow velocity was four to five orders of magnitude greater than the rate expected from the Hagen–Poiseuille equation governing macroscale hydrodynamics [48]. A research report notes another fluid flow experiment based on a CNT membrane synthesized with the help of nanofabrication methodologies (**Figure 7(a)**). This type of membrane had a double-wall CNTs with <2-nm diameter and exhibited flow velocity rates of three to four orders of magnitude greater than the values calculated theoretically [49].

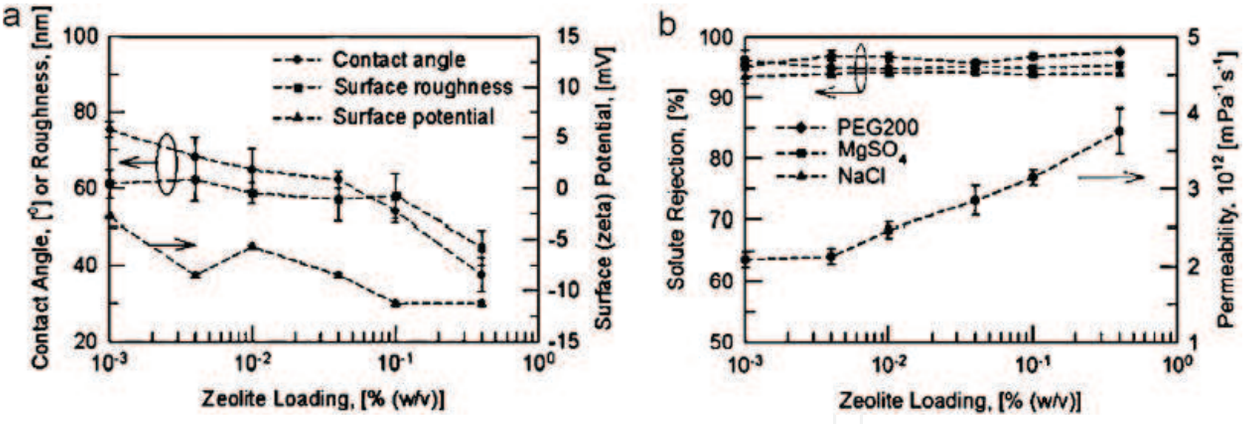

Figure 6. Effect of zeolite-loading dosage on (a) surface properties and (b) separation performance (reprinted with permission from Jeong et al. [44]).

A new investigation focused on the water transport potential passing through template-grown car bon nanopipes (CNPs) of around 44 nm in diameter. In this case, the CNPs were designed based on non-catalytic CVD that yield an amorphous, or turbostratic, graphitic structure (**Figure 7(b)**). The existence of the template helps eliminate structural imperfections, from tortuosity, and including, to branching and pore misalignment. However, the flow enhancement factor of over the theoretically predicted value is around 20, which is substantially less than was observed in earlier cases [50]. Researchers argue that this is caused by the varying structure and surface chemistry, if compared to the CNTs described in the previous articles and prepared by CVD.

A number of ongoing scientific discussions have emerged from the experimental results showcasing fast water transport [46, 51, 52]. The critical source of this exceptionally fast water transport in CNTs is not entirely defined and multiple, often contradictory, justifications have been observed in studies exploring this property [53–55]. One of the explanations suggests that the formation of a robust hydrogen-bonding network between atomically smooth hydrophobic inner nanotube wall and water molecules can facilitate spontaneous inhibition. This in turn leads to the creation of a vapor layer between the surface and the bulk flow, the latter responsible for water transport in a projected flow [56, 57]. Alternatively, an argument can be made that the frictionless water flow is caused by the creation of a layer of liquid water molecules on the CNT walls. This layer can in theory offer a type of "shielding" to the bulk water molecules in a way that forces them to flow at a faster rate [58].

The ion transport through CNT channels has been examined from, both, computational and experimental angles. Transport of ions with different valences has been assessed in double-walled-type CNTs of 1–2-nm diameter and functionalized with negatively charged groups. Despite the ion rejection potential not being suitably high for the purposes of desalination, this research study suggests that CNTs' ion exclusion mechanism is controlled by electrostatic interactions (Donnan exclusion), instead of the steric effects. This analysis is grounded in the conclusion that the electrostatic screening length and solution pH considerably alter the ion rejection potential [49, 59]. Majumder's group also showed two specific methods of changing the selectivity of various ion species, specifically, the pore size modification using CNT tip functionalization and the voltage-based gate control approach [60, 61]. While the monovalent salt rejection potential is not verified in both instances, these research studies illustrate the potential of effectively

http://dx.doi.org/10.5772/intechopen.71719

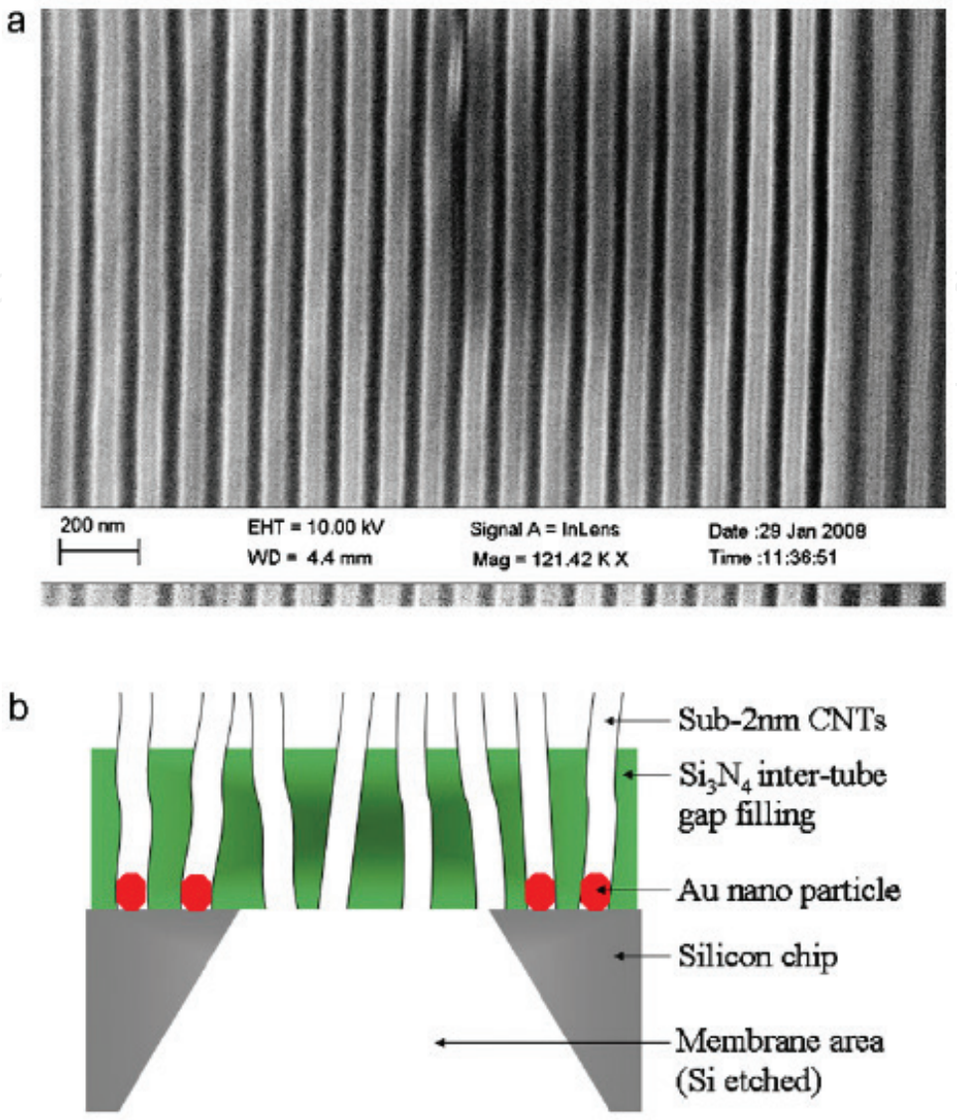

Figure 7. (a) Schematic of CNT membrane reported in [49]; and (b) SEM micrograph showing cross-section of CNP membrane [50].

altering pore characteristics and as a consequence improving selectivity. A molecular dynamic simulation run based on RO using CNTs has been conducted in connection to the physical size exclusion mechanisms. This experiment-based testing indicated that 0.8-nm CNTs can entirely reject the salt, while at the same time offer at least a fourfold flux enhancement over the current high-quality TFC RO membranes, and contingent on the expected CNT packing density values [62, 63]. This simulation did not consider the influence of charge functionalities that frequently occur at both ends of CNTs. Their occurrence may be capable of expanding the CNT size regime, since the creation of charge double layer could help raise the total salt rejection values [51].

Mauter and Elimelech combined the preceding desalination developments in CNT membranes in order to prepare the key data for the next generation in CNT membrane production [2]. Their study suggests that although CNT membranes are a highly encouraging area of research when it comes to flux improvement, a substantially more in-depth research work is necessary for the successful creation of synthesis methodologies. In particular, they

argue that there is a need for synthesis methodologies that would be able to align arrays of single-walled CNTs with sub-nanometer diameters, as well as improve tip functionalization and offer a more effective salt rejection potential. The creation of the CNT/polymeric membranes from the experimental studies outlined above [47–49], and in various other gas separation studies, requires a multiplicity of complex steps, including polymer filling of the inter-tube spaces, substrate removal, catalytic growth of CNTs onto expensive substrates, and CNT tip opening using etching. Moreover, the CNT diameter size distribution is not small enough to align with the simulation studies being conducted. To transcend these concerns, a patent has revealed a dynamic where there is a mixing of CNTs into solutions, primarily crosslinking agent solutions like trimesoyl of isophthalic chlorides, for the construction of successful composite polymeric membranes (**Figure 8**). This alternative option may ensure that the CNTs can be efficiently fixed into the barrier layer created using conventional interfacial polymerization on a micro-porous polyethersulfone support [64]. In this instance, the CNTs must be functionalized in order to ensure improved organic solvent solubility, and in this particular patent the CNTs are functionalized with octadecylamine. The membrane design in this manner can be effortlessly customized for RO systems and current filtration needs, with the CNTs measuring 0.8 nm in diameter. The water then permeates through the membrane by, both, the embedded CNT pathways and the conventional polymeric barrier layer. A test revealed as part of the patent shows a comparison between membranes developed with and without embedded CNTs, so as to illustrate the improved flow capacity achieved using the CNT pathways. With CNTs present in the experiment, a marginally higher salt rejection potential was obtained (97.69% as compared with 96.19%), as well as an almost a doubled water flux value (44 L m^{-2} day^{-1} bar^{-1} as compared with 26 L m^{-2} day^{-1} bar^{-1}). Although the resulting data are highly encouraging, the synthesized membrane disc was only 47 mm in diameter and as such still leaves a research gap. Extended

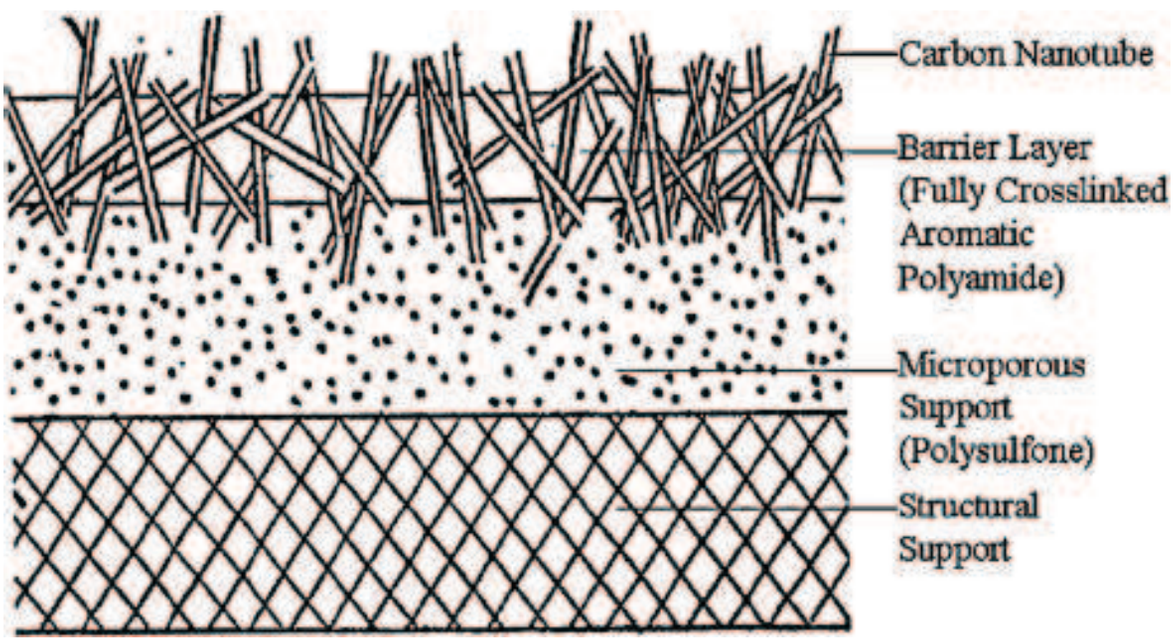

Figure 8. Schematic cross-section of CNTs-embedded TFC membrane [64].

studies using membranes with much larger surface areas are needed before large-scale manufacturing methodologies can be successfully established, tested, and implemented.

5. Development of robust organosilica membranes for reverse osmosis

The hybrid organically bridged silica membranes have attracted considerable attention due to their successful performances in a variety of applications. The development of robust reverse osmosis membranes that can withstand aggressive operating conditions is still a major challenge. A new type of microporous organosilica membrane has been developed and applied in reverse osmosis. Sol–gel-derived organosilica RO membranes reject isopropanol with a rejection potential higher than 95%, demonstrating superior molecular-sieving ability for neutral solutes of low-molecular weight. Due to the introduction of an inherently stable hybrid network structure, this membrane withstands higher temperatures in comparison to the commercial polyamide RO membranes and is resistant to water to at least 90°C with no obvious changes in its filtration performance. Furthermore, both an accelerated chlorine-resistance test and Fourier transform infrared analysis confirm excellent chlorine stability for this material, a quality that demonstrates promise for a new generation of chlorine-resistant RO membrane materials [65]. Organosilica membranes were prepared using the sol–gel technique via a polymeric route with $(EtO)_3Si\text{-}CH_2CH_2\text{-}Si(OEt)_3$ (BTESE) as a single precursor. The synthesis of nanometer-sized BTESE polymer sol was performed as previously reported [66]. The organosilica membrane composition is presented in **Figures 9** and **10**.

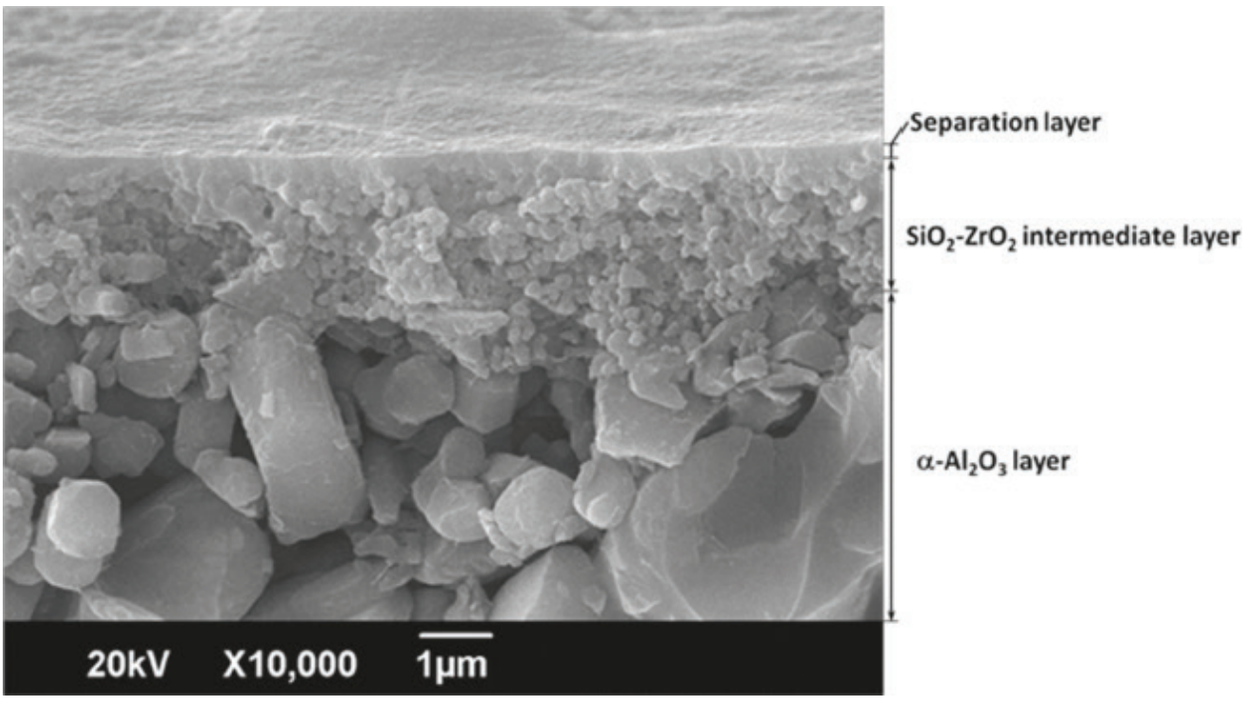

Figure 9. Cross-sectional SEM image of the BTESE-derived organosilica membrane [66]; Copyright 2011, Journal of Membrane Science.

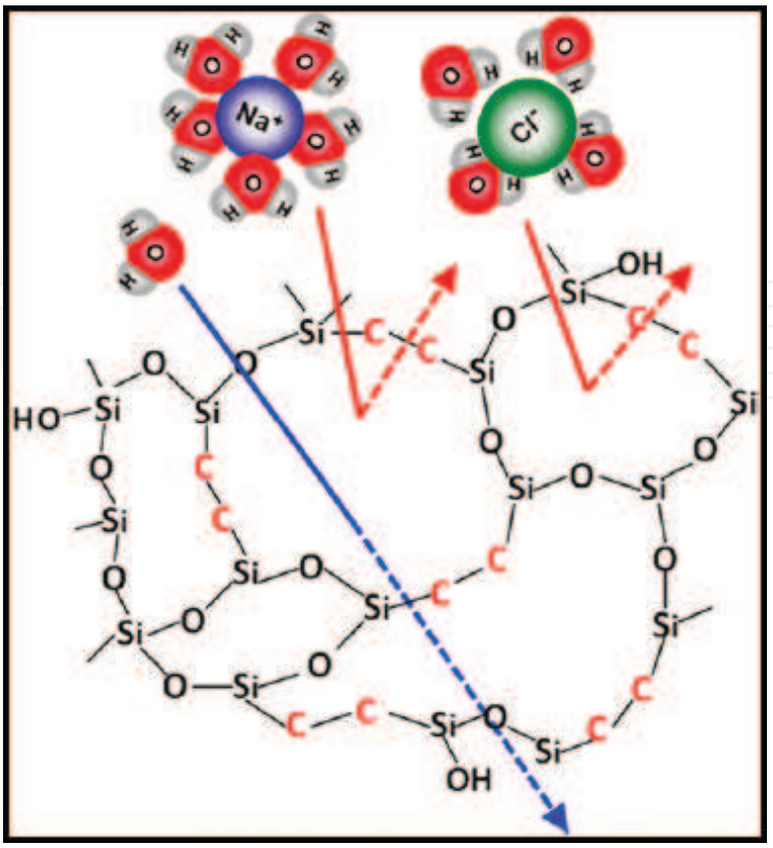

Figure 10. Hybrid organically bridged silica membranes [66]; Copyright 2011, Journal of Membrane Science.

The organosilica membranes derived from BTESE exhibit superior molecular-sieving abilities for neutral solutes of low-molecular weight. Exceptional hydrothermal stability has been obtained due to the introduction of an inherently stable, organically bridged silica network structure, significantly broadening the application fields of the organosilica membranes. Furthermore, these organosilica RO membranes already show excellent chlorine stability under a wide range of chlorine concentrations. For example, after a total chlorine exposure of up to 35,000 ppm for 3 h, there was no noticeable change in separation performance.

6. Biomimetic RO membranes

Superior water transport characteristics found in biological membranes have directed researchers toward the study of membranes that incorporate aquaporins or proteins acting as water-selective channels in biological cell membranes [67]. Membranes that include bacterial aquaporin Z proteins have been shown to offer enhanced water transport capabilities if compared to conventional RO membranes [68]. For example, aquaporins have been integrated into the walls of self-assembled polymer vesicles consisting of triblock copolymer, poly(2-methyl-2-oxazoline)-block-poly(dimethylsiloxane)-block-poly(2-methyl-2-oxazoline). Stopped-flow light-scattering experiments were carried out as an initial permeability test for the aquaporin-triblock polymer vesicles. The experimental data from this test indicate that there was at least

one order of magnitude detected in permeability improvement, if compared to the standard commercially available TFC RO-type membranes [68]. While a salt separation test was not included in the experiment, an exceedingly high salt rejection potential is anticipated from the aquaporins due to their functional biological performance, which only permits the passage of water molecules. As a result, these conditions embody a superior prospect for the creation of ultra pure water [68–70]. Studies such as these have a narrow focus that limits them to examining water permeability properties through a barrier layer composed of triblock polymers and aquaporins. Numerous key issues, including the understanding of the membrane's fouling resistance, identifying appropriate support materials, and locating the suitable range of operating conditions, have to be dealt with before this membrane can be effectively developed for industrial and practical applications. The relevance of the NF membranes as a biomimetic membrane support has been likewise observed [71]. By applying the vesicle fusion approach, a continuous phospholipid bilayer was formed on an NTR-7450 and was able to fully cover the membrane. Additional research studies must be undertaken with the aim to include aquaporins into the phospholipid bilayer for practical applications in water purification processes. In Denmark in 2005, a company Aquaporin was formed specifically to advance these membranes for long-term industrial applications. The company has recently received a patent for the methodology of building membranes that successfully include aquaporins (**Figure 11**) [72]. As part of this patented approach, instead of using triblock polymers, the aquaporins are reorganized into lipid bilayers developed with the help of the Langmuir–Blodgett method, using spin coating, or vesicle fusion method. Aquaporin's patent likewise notes two distinct membrane orientations: (1) first orientation where a lipid bilayer including the aquaporins is inserted between two hydrophilic porous support layers, like polysulfone, cellulose, or mica; and (2) second orientation where a lipid bilayer including aquaporins is constructed over a hydrophobic porous support membrane, like the porous PTFE film. Although severe concentration polarization and fouling are reported, the patent does not offer significant numerical data with regard to the membrane's salt rejection and flux potential values.

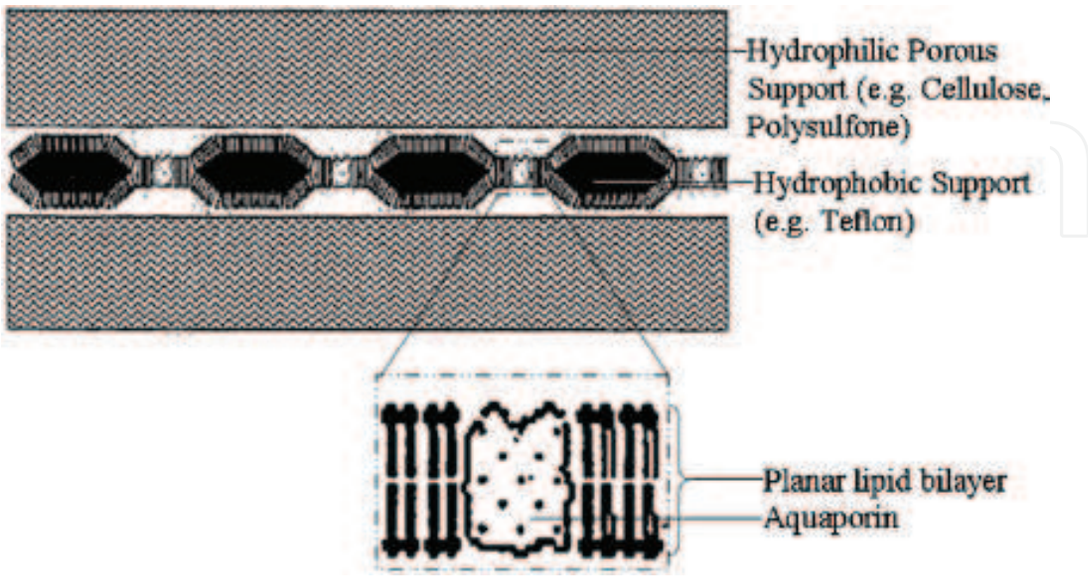

Figure 11: Schematic cross section of aquaporin-embedded membrane [72].

Author details

Amira Abdelrasoul[1]*, Huu Doan[2] and Ali Lohi[2]

*Address all correspondence to: amira.abdelrasoul@usask.ca

1 Department of Chemical and Biological Engineering, University of Saskatchewan, Saskatoon, Saskatchewan, Canada

2 Department of Chemical Engineering, Ryerson University, Toronto, Ontario, Canada

References

[1] Li D, Wang H. Recent developments in reverse osmosis desalination membranes. JMCh. 2010;**20**:4551-4566

[2] Mauter MS, Elimelech M. Environmental applications of carbon-based nanomaterials. Environmental Science & Technology. 2008;**42**:5843-5859

[3] Lu Y, Suzuki T, Zhang W, Moore JS, Mariñas BJ. Nanofiltration membranes based on rigid star amphiphiles. Chemistry of Materials. 2007;**19**:3194-3204

[4] Suzuki T, Lu Y, Zhang W, Moore JS, Mariñas BJ. Performance characterization of nanofiltration membranes based on rigid star amphiphiles. Environmental Science & Technology. 2007;**41**:6246-6252

[5] Siskens CAM. Applications of ceramic membranes in liquid filtration. In: Burggraaf AJ, Cot L, editors. Membrane Science and Technology. Elsevier; 1996. Vol. **13**. p. 619-639

[6] Pabby AK, Rizvi SSH, Sastre AM. Handbook of Membrane Separations: Chemical, Pharmaceutical Food and Biotechnological Applications. Boca Raton: CRC Press; 2009

[7] Gazagnes L, Cerneaux S, Persin M, Prouzet E, Larbot A. Desalination of sodium chloride solutions and seawater with hydrophobic ceramic membranes. Desalination. 2007;**217**:260-266

[8] Duke MC, Mee S, da Costa JCD. Performance of porous inorganic membranes in non-osmotic desalination. Water Research 2007;**41**:3998-4004.

[9] Kujawski W, Krajewska S, Kujawski M, Gazagnes L, Larbot A, Persin M. Pervaporation properties of fluoroalkylsilane (Fas) grafted ceramic membranes. Desalination. 2007; **205**:75-86

[10] Lia L, Dong J, Nenoff TM, Lee R. Reverse osmosis of ionic aqueous solutions on Amfi zeolite membrane. Desalination. 2004;**170**:309-316

[11] Lin J, Murad S. A computer simulation study of the separation of aqueous solutions using thin zeolite membranes. Molecular Physics: An International Journal at the Interface Between Chemistry and Physics. 2001;**99**:1175-1181

[12] Baerlocher C, McCusker LB, Olson DH. Atlas of Zeolite Framework Types. 6th ed. Amsterdam: Elsevier; 2007

[13] Li L, Dong J, Nenoff TM, Lee R. Desalination by reverse osmosis using Mfi zeolite membranes. Journal of Membrane Science. 2004;**243**:401-404

[14] Jareman F, Hedlund J, Sterte J. Effects of aluminum content on the separation properties of Mfi membranes. Separation and Purification Technology. 2003;**32**:159-163

[15] Duke MC, O'Brien-Abraham J, Milne N, Zhu B, Lin JYS, Diniz da Costa JC. Seawater desalination performance of Mfi type membranes made by secondary growth. Separation and Purification Technology. 2009;**68**:343-350

[16] Li L, Liu N, McPherson B, Lee R. Enhanced water permeation of reverse osmosis through Mfi-type zeolite membranes with high aluminum contents. Industrial & Engineering Chemistry Research. 2007;**46**:1584-1589

[17] Liu N, Li L, McPherson B, Lee R. Removal of organics from produced water by reverse osmosis using Mfi-type zeolite membranes. Journal of Membrane Science. 2008;**325**:357-361

[18] Lu J, Liu N, Li L, Lee R. Organic fouling and regeneration of zeolite membrane in wastewater treatment. Separation and Purification Technology. 2010;**72**(2):203-207

[19] Gogotsi Y, Nikitin A, Ye H, Zhou W, Fischer JE, Yi B, Foley HC, Barsoum MW. Nanoporous carbide-derived carbon with tunable pore size. Nature Materials. 2003;**2**:591-594

[20] Hoffman EN, Yushin G, Wendler BG, Barsoum MW, Gogotsi Y. Carbidederived carbon membrane. MCP. 2008;**112**:587-591

[21] Kulprathipanja S, Neuzil RW, Li NN. Separation of Fluids by Means of Mixed Matrix Membranes, Patent Application No. 4740219 1988

[22] Okumus E, Gurkan T, Yilmaz L. Development of a mixed-matrix membrane for pervaporation. Separation Science and Technology. 1994;**29**:2451-2473

[23] Ismail AF, Goh PS, Sanip SM, Aziz M. Transport and separation properties of carbon nanotube-mixed matrix membrane. Separation and Purification Technology. 2009;**70**(1):12-26

[24] Nga LY, Mohammada AW, Leob CP, Hilal N. Polymeric membranes incorporated with metal/metal oxide nanoparticles: A comprehensive review. Desalination. 2013;**308**:15-33

[25] Gribov EN, Parkhomchuk EV, Krivobokov IM, Darr JA, Okunev AG. Journal of Membrane Science. 2007;**297**:1

[26] Arico AS, Baglio V, Di Blasi A, Antonucci V. Electrochemistry Communications. 2003;**5**:862

[27] Arico AS, Baglio V, Di Blasi A, Creti P, Antonucci PL, Antonucci V. Solid State Ionics. 2003;**161**:251

[28] Lee K, Nam JH, Lee JH, Lee Y, Cho SM, Jung CH, Choi HG, Chang YY, Kwon YU, Nam JD. Electrochemistry Communications. 2005;**7**:113

[29] Baglio V, Arico AS, Di Blasi A, Antonucci V, Antonucci PL, Licoccia S, Traversa E, Fiory FS. Electrochimica Acta. 2005;**50**:1241

[30] Bauer F, Willert-Porada M. Journal of Membrane Science. 2004;**233**:141

[31] Lin CW, Fan KC, Thangamuthu R. Journal of Membrane Science. 2006;**278**:437

[32] Daiko Y, Klein LC, Kasuga T, Nogami M. Journal of Membrane Science. 2006;**281**:619

[33] Xu W, Lu T, Liu C, Xing W. Electrochimica Acta. 2005;**50**:3280

[34] Jalani NH, Dunn K, Datta R. Electrochimica Acta. 2005;**51**:553

[35] Ren S, Sun G, Li C, Liang Z, Wu Z, Jin W, Qin X, Yang X. Journal of Membrane Science. 2006;**282**:450

[36] Chen Z, Holmberg B, Li W, Wang X, Deng W, Munoz R, Yan Y. Chemistry of Materials. 2006;**18**:5669

[37] Gao J, Lee D, Yang Y, Holdcroft S, Frisken BJ. Macromolecules. 2005;**38**:5854

[38] Brijmohan SB, Shaw MT. Journal of Membrane Science. 2007;**303**:64

[39] Ramirez LP, Landfester K. Macromolecular Chemistry and Physics. 2003;**204**:22

[40] Gasa JV, Boob S, Weiss RA, Shaw MT. Journal of Membrane Science. 2006;**269**:177

[41] Sunada K, Kikuchi Y, Hashimoto K, Fujishima A. Bactericidal and detoxification effects of TiO2 thin film photocatalysts. Environmental Science & Technology. 1998;**32**:726-728

[42] Kim SH, Kwak SY, Sohn BH, Park TH. Design of TiO_2 nanoparticle selfassembled aromatic polyamide thin-film-composite (TFC) membrane as an approach to solve biofouling problem. Journal of Membrane Science. 2003;**211**:157-165

[43] Kwak SY, Kim SH, Kim SS. Hybrid organic/inorganic reverse osmosis (RO) membrane for bactericidal anti-fouling. 1. Preparation and characterization of TiO2 nanoparticle self-assembled aromatic polyamide thin-film-composite (TFC) membrane. Environmental Science & Technology. 2001;**35**:2388-2394

[44] Jeong BH, Hoek EMV, Yan Y, Subramani A, Huang X, Hurwitz G, Ghosh AK, Jawor A. Interfacial polymerization of thin film nanocomposites: A new concept for reverse osmosis membranes. Journal of Membrane Science. 2007;**294**:1-7

[45] Lind ML, Ghosh AK, Jawor A, Huang X, Hou W, Yang Y, Hoek EMV. Influence of zeolite crystal size on zeolite-polyamide thin film nanocomposite membranes. Langmuir. 2009;**25**:10139-10145

[46] Noy A, Park HG, Fornasiero F, Holt JK, Grigoropoulos CP, Bakajin O. Nanofluidics in carbon nanotubes. Nano Today. 2007;**2**:22-29

[47] Hinds BJ, Chopra N, Rantell T, Andrews R, Gavalas V, Bachas LG. Aligned multiwalled carbon nanotube membranes. Sci. 2004;**303**:62-65

[48] Majumder M, Chopra N, Andrews R, Hinds BJ. Nanoscale hydrodynamics: Enhanced flow in carbon nanotubes. Nature. 2005;**438**:44

[49] Holt JK, Park HG, Wang Y, Stadermann M, Artyukhin AB, Grigoropoulos CP, Noy A, Bakajin O. Fast mass transport through Sub-2-nanometer carbon nanotubes. Science. 2006;**312**:1034-1037

[50] Whitby M, Cagnon L, Thanou M, Quirke N. Enhanced fluid flow through nanoscale carbon pipes. Nano Letters. 2008;**8**:2632-2637

[51] Holt JK. Carbon nanotubes and nanofluidic transport. Advanced Materials. 2009;**21**: 3542-3550

[52] Mattia D, Gogotsi Y. Review: Static and dynamic behavior of liquids inside carbon nanotubes. Microfluidics and Nanofluidics. 2008;**5**:289-305

[53] Striolo A. The mechanism of water diffusion in narrow carbon nanotubes. Nano Letters. 2006;**6**:633-639

[54] Joseph S, Aluru NR. Why are carbon nanotubes fast transporters of water? Nano Letters. 2008;**8**:452-458

[55] Thomas JA, McGaughey AJH. Reassessing fast water transport through carbon nanotubes. Nano Letters. 2008;**8**:2788-2793

[56] Hummer G, Rasaiah JC, Noworyta JP. Water conduction through the hydrophobic channel of a carbon nanotube. Nature. 2001;**414**:188-190

[57] Kalra A, Garde S, Hummer G. Osmotic water transport through carbon nanotubes membranes. PNAS. 2003;**100**:10175-10180

[58] Kotsalis EM, Walther JH, Koumoutsakos P. Multiphase water flow inside carbon nanotubes. International Journal of Multiphase Flow. 2004;**30**:995-1010

[59] Francesco Fornasieroa HGP, Holta JK, Stadermanna M, Costas P, Grigoropoulosc NA, Bakajina O. Ion exclusion by sub- 2-nm carbon nanotube pores. Proceedings of the National Academy of Sciences of the United States of America. 2008;**105**:17250-17255

[60] Majumder M, Chopra N, Hinds BJ. Effect of tip functionalization on transport through vertically oriented carbon nanotube membranes. Journal of the American Chemical Society. 2005;**127**:9062-9070

[61] Majumder M, Zhan X, Andrews R, Hinds BJ. Voltage gated carbon nanotube membranes. Langmuir. 2007;**23**:8624-8631

[62] Corry B. Designing carbon nanotube membranes for efficient water desalination. The Journal of Physical Chemistry B. 2007;**112**:1427-1434

[63] Suk ME, Raghunathan AV, Aluru NR. Fast reverse osmosis using boron nitride and carbon nanotubes. Applied Physics Letters. 2008;**92**:133120

[64] Ratto TV, Holt JK, Szmodis AW. Membranes with Embedded Nanotubes for Selective Permeability patent application No. 20100025330 2010

[65] Subramani A, Voutchkovb N, Jacangelo JG. Desalination energy minimization using thin film nanocomposite membranes. Desalination. 2014;**350**:35-43

[66] Lee KP, Arnot TC, Mattia D. A review of reverse osmosis membrane materials for desalination—Development to date and future potential. Journal of Membrane Science. 2011;**370**:1-22

[67] Agre P. Membrane water transport and aquaporins: Looking back. Biology of the Cell. 2005;**97**:355-356

[68] Kumar M, Grzelakowski M, Zilles J, Clark M, Meier W. Highly permeable polymeric membranes based on the incorporation of the functional water channel protein aquaporin Z. PNAS. 2007;**104**:20719-20724

[69] Gonzaˇılez-Peˇırez A, Stibius KB, Vissing T, Nielsen CH, Mouritsen OG. Biomimetic triblock copolymer membrane arrays: A stable template for functional membrane proteins. Langmuir. 2009;**25**:10447-10450

[70] Taubert A. Controlling water transport through artificial polymer/protein hybrid membranes. PNAS. 2007;**104**:20643-20644

[71] Kaufman Y, Berman A, Freger V. Supported lipid bilayer membranes for water purification by reverse osmosis. Langmuir. 2010;**26**:7388-7395

[72] Jensen PH, Keller D, Nielsen CH. Membrane for Filtering of Water. Patent Application No. EP1885477 2010